LATTICE BOLTZMANN SIMULATION OF RESISTANCE COEFFICIENT OF THE OIL AND WATER MIGRATION IN POROUS MEDIA

by

Han-Bing QI [a,b]***, Dong-Hai LI*** [a]***, Wei WEI*** [a]***, Xin-Hao HU*** [a]***,***
Dong LI [a,b*]***, Guo-Zhong WU*** [a]***, and Xiao-Yan LIU*** [a]

[a] School of Civil and Architectural Engineering, Northeast Petroleum University, Heilongjiang Province, Heilongjiang, China
[b] Heilongjiang Key Laboratory of Petroleum and Petrochemical Multiphase Treatment and Pollution Prevention, Heilongjiang Province, Heilongjiang, China

Original scientific paper
https://doi.org/10.2298/TSCI171011039Q

The coefficients of oil and water transfer resistance in porous media are the basis of numerical study on the migration of contamination in the pipeline, soil cleaning, oilfield water flooding, and oilfield water treatment. Based on the quartet structure generation set, the porous media with random distribution are constructed. The lattice Boltzmann method is used to simulate the mesoscopic migration of oil and water in porous media. Then the distribution law of oil and water velocity and pressure in porous media is analyzed, and the fitting equations of oil and water resistance coefficients are obtained under different porosity. The results show that when the oil and water migrate in porous media, the viscous resistance coefficient is larger than the inertia resistance factor, and the viscosity resistance coefficient of water is obviously higher than that of oil, while the coefficient of inertia resistance of oil and water is nearly same.

Key words: *porous media, mesoscopic migration, resistance coefficient, lattice Boltzmann model*

Introduction

The coefficients of viscous drag and inertia resistance are the key parameters for the flow of liquid medium in porous media, such as leaking pollutant migration of oil pipeline in soil [1], contaminated soil cleaning [2], oilfield flooding [3], and oilfield water treatment [4].

A large number of studies on the flow of fluid in porous media have been carried out, and corresponding computational models have also been developed. For example, the resistance characteristics of porous media were simulated by using glass ball [5]. The simulation of two-phase flow in porous media was investigated by using the simulation method, based on the porous media theory and the capillary hysteretic internal variable mode [6]. A channel model of particle filled porous media was established, and the resistance characteristics of single-phase water adiabatic flow were numerically simulated [7]. Boltzmann simulation method was more suitable for the realization and research of micro-structure of porous structure [8-12]. For exam-

*Corresponding author, e-mail: lidonglvyan@126.com

ple, permeability of porous media was calculated using Boltzmann model [13], and a lattice Boltzmann method was used to simulate the boundary between the porous structure of the solid and the fluid [14]. The stated studies show that the resistance coefficient of porous media is very important for the study of the flow of spheres in porous media, however, there are few literatures about the relationship between the coefficients of oil and water migration resistance in porous media.

In this paper, the flow resistance characteristics of oil and water in porous media were studied, and porous media were constructed by Quartet Structure Generation Set. Based on the Boltzmann method, mesoscopic simulation of oil and water medium flow in porous media with different porosity under different driving pressure was carried out. In the later stage, the resistance coefficients of porous media with different porosity were obtained by fitting the driving pressure with the flow average velocity. The curves of the viscous resistance coefficient and the inertia resistance coefficient with the porosity were fitted, and the corresponding equations were obtained. Finally, the variation law of the resistance coefficient was analyzed.

Method

Physical and mathematical models

A small area (0.002 mm × 0.002 mm) in a porous medium is selected. The 2-D physical model of oil and water migration in porous media is shown in fig. 1. Among them, the ADEH region is the computational area (lattice number 200 × 200). The left boundary AH is high concentration boundary. The right boundary DE is the low concentration boundary, and boundaries EH and AD are impermeable. The BCFG region is filled with porous media, and the ABGH and CDEF zones are buffers. Where W is the width of the buffer, ε is the porous media porosity was put in front of the direction of oil and water migration is from left to right in porous media. Simulation conditions are shown in tab. 1.

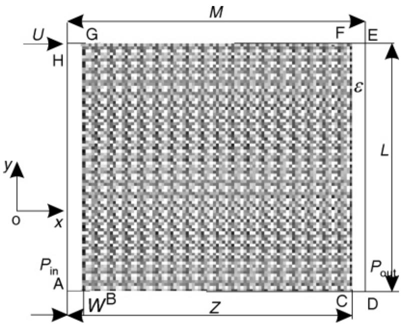

Figure 1. Physical model

Table 1. Simulation conditions

L	M	W	Z	P_{in}	P_{out}	ε	U
200	200	5	190	1.001/1.01/1.05/1.1	1	0.5/0.6/0.7/0.8/0.9	0.001

The standard collision migration rules and lattice units are employed in this simulation. At the same time, the time step and the grid step length are both 1, $\partial t = \partial x = \partial y = 1$. As can be seen from the conditions, the density of the grid is equal to 1.

Simulation conditions of regional boundary setting are: upper boundar $u = 0$, lower boundary $u = 0$, left boundary $U = 0.001$, $P = P_{\text{in}}$, right boundary $P = P_{\text{out}}$, solid boundary of porous media $\partial u/\partial n = 0$.

Lattice Boltzmann model

The lattice Boltzmann model is employed in the D2G9 model [15]. The evolution equation of the density distribution function is:

$$f_i(r \quad e_i\Delta t, t \quad \Delta t) \quad f_i(r,t) \qquad \frac{1}{\tau_f}[f_i(r,t) \quad f_i^{\text{eq}}(r,t)] \tag{1}$$

where e_i applies the discrete velocity model of D2Q9, τ_f – the dimensionless time, and f_i^eq – the density equilibrium distribution function. The calculation parameters are given:

$$f_i^{\mathrm{eq}} \quad \begin{matrix} 4d_0 \dfrac{p}{c^2} \quad S_i(u) & i \quad 0 \\ d_1 \dfrac{p}{c^2} \quad S_i(u) & i \quad 1,2,3,4 \\ d_2 \dfrac{p}{c^2} \quad S_i(u) & i \quad 5,6,7,8 \end{matrix} \tag{2}$$

$$S_i(u) \quad \omega_i \quad \frac{e_i u}{c_s^2} \quad \frac{(e_i u)^2}{2c_s^4} \quad \frac{u^2}{2c_s^2} \qquad i \quad 1,2,3,4,5,6,7,8 \tag{3}$$

where c is the lattice velocity, u – the fluid velocity, P – the pressure, and d_0, d_1, d_2 must meet $d_1 + d_2 = d_0$ and $d_1 + 2\,d_2 = 1/2$. Assumed $d_0 = 5/12$, $d_1 = 1/3$, $d_2 = 1/12$.

$$e_i \quad \begin{matrix} (0,0) & i=0 \\ (\cos[(i \quad 1)\pi/2, \sin[(i \quad 1)\pi/2])c & i \quad 1,2,3,4 \\ \sqrt{2}(\cos[(i \quad 5)\pi/2 \quad \pi/4], \sin[(i \quad 5)\pi/2 \quad \pi/4])c & i \quad 5,6,7,8 \end{matrix} \tag{4}$$

where e_i is the discrete velocity, the weight coefficients are $\omega_0 = 4/9$, $\omega_{1\text{-}4} = 1/9$, $\omega_{5\text{-}8} = 1/36$, $c_s^2 = c^2/3$.

The velocity and pressure of a fluid are calculated:

$$u \quad {}_i e_i f_i \tag{5}$$

$$P \quad \rho_0 \frac{c^2}{4d_0}[\ {}_{i \ 0} f_i \quad s_0(u)] \tag{6}$$

The macroscopic governing equations of fluid can be derived as

$$u \quad 0 \tag{7}$$

$$\frac{\partial u}{\partial u} \quad (uu) \quad \frac{P}{\rho_0} \quad v \quad {}^2 u \tag{8}$$

$$v \quad c_s^2 \ \tau_f \quad \frac{1}{2} \ \delta_t \tag{9}$$

The model's four boundaries are treated with the non-equilibrium extrapolation scheme and two order accuracy proposed by [16]. Then the boundary of solid particles in porous media region adopts the rebound scheme proposed by [17]. The convergence criterion is given:

$$u_{\mathrm{error}} \quad \frac{\sqrt{\ {}_{i,j}\{[u_x(i,j,t \quad \delta_t) \quad u_x(i,j,t)]^2 \quad [u_y(i,j,t \quad \delta_t) \quad u_y(i,j,t)]^2\}}}{\sqrt{\ {}_{i,j}[u_x(i,j,t \quad \delta_t)]^2 \quad [u_y(i,j,t \quad \delta_t)]^2}} \quad \eta \tag{10}$$

where η is a small amount which is 10^{-6}.

Resistance coefficient acquisition model

For the limit in high velocity flow, it is necessary to extend Darcy's law. The viscous resistance and the inertia resistance should be considered in the expansion. The coefficient of resistance is obtained by using the binomial law of seepage.

$$\Delta P \quad a_1 v \quad a_2 v^2 \tag{11}$$

$$\frac{\Delta P}{\Delta n} \quad S_i \tag{12}$$

$$\frac{1}{\alpha} \quad \frac{\alpha_1}{\mu \quad n} \tag{13}$$

$$C_2 \quad \frac{2\alpha_2}{\rho \quad n} \tag{14}$$

where P is the pressure drop for a fluid passing through a porous medium, v – the flow velocity, a_1 and a_2 are the fitting coefficient, n – the thickness of the porous medium, $1/\alpha$ – the coefficient of viscous resistance, and C_2 – the coefficient of inertia resistance.

Results and discussion

Random distribution porous media with porosity 0.5/0.6/0.7/0.8/0.9 are constructed. The simulation is carried out when the pressure difference is 0.001/0.01/0.05/0.1. The oil and water density are 838.8 and 998.2 kg/m^3, respectively. The viscosity of oil and water is 0.008832 and 0.001003, kgm/s, respectively.

Porous medium

The porous media are generated by the random Quartet Structure Generation Set [18]. The growth rate of solid growth nucleation is selected 0.01, and growth kernel distribution is 0.01. Figure 2 shows porous media structure diagram with porosity of 0.5/0.6/0.7/0.8/0.9.

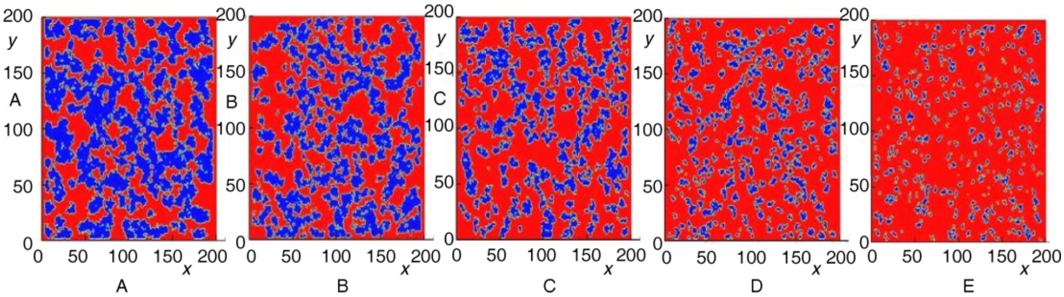

Figure 2. Porous media structure diagram; A – 0.5, B – 0.6, C – 0.7, D – 0.8, E – 0.9

Mesoscopic migration characteristics of oil and water

Porous media porosity 0.5/0.6/0.7/0.8/0.9 and the simulated drive pressure difference 0.001/0.01/0.05/0.1 are selected. Through the transformation between the grid unit and the physical unit, water migration physical pressure is 0.362801797/3.628017971/18.14008986/36.28017971, Pa, and oil migration physical pressure is 33.47686864/334.7686864/1673.843432/3347.686864, Pa. In this paper, the velocity profiles and pressure profiles of porous media and streamline profiles are used to compare the results of oil and water.

Figure 3 shows the velocity profiles of oil and water migration in porous media, when the pressure difference is 0.001/0.01/0.05/0.1 and the porosity is 0.6. The blue region is the solid

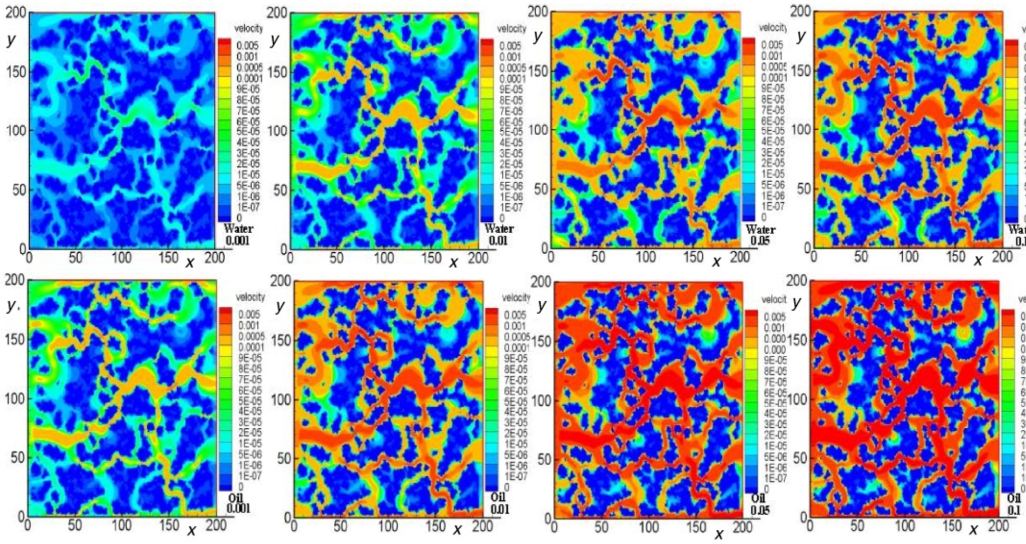

Figure 3. Water and oil velocity profiles at different pressure difference

structure of porous medium. As can be seen that the oil and water migration in porous media has many main stream from left boundary to right boundary, and the main distribution of different pressure difference of porous media is the same. The position ($x = 152$, $y = 109$) of the maximum velocity point of oil and water migration in porous media is consistent. In porous media, velocity does not change from large to small along the direction of flow. It is larger in smaller pores, but smaller in larger pores. The velocity of some pore area in the porous medium is 0 when the pressure is small, which indicates that it is necessary to have a critical pressure of oil and water movement in porous medium when the fluid filled with all voids. The distribution of oil and water at different pressure gradients, and the overall distribution of the velocity are approximately similar, but the velocity increases with the increase of pressure, which shows that the distribution of oil and water migration velocity is determined by the structure and pressure of the porous medium. The average velocity, the maximum velocity and the average velocity of the outlet face are obtained from the simulation in figs. 4-6.

As shown in velocity curves 4-6 at differential pressure difference of the oil and water, it can be seen that the average velocity and maximum velocity of export terminal increase, with the increase of pressure.

Figure 7 shows the pressure profiles of oil and water migration in porous media when the pressure difference is 0.001/0.01/0.05/0.1 and the porosity is 0.6, and the blue region is the solid structure of porous medium. From the distribution of pressure nephogram, as the oil and water flow in the porous medium, the pressure of enclosed pore (light blue part) does not change with the pressure between the two sides. The pressure in porous media decreases along the direction of fluid-flow, and the pressure distribution is related to the pore structure of porous media. Under different pressure gradient, the pressure distribution of oil and water in porous media is similar. In the porous medium, the solid structure is randomly distributed, and the porous cavity with different shapes can be formed, and the entrance and exit of many cavities are connected with each other, thus forming the whole structure of the porous medium. For a single cavity, the

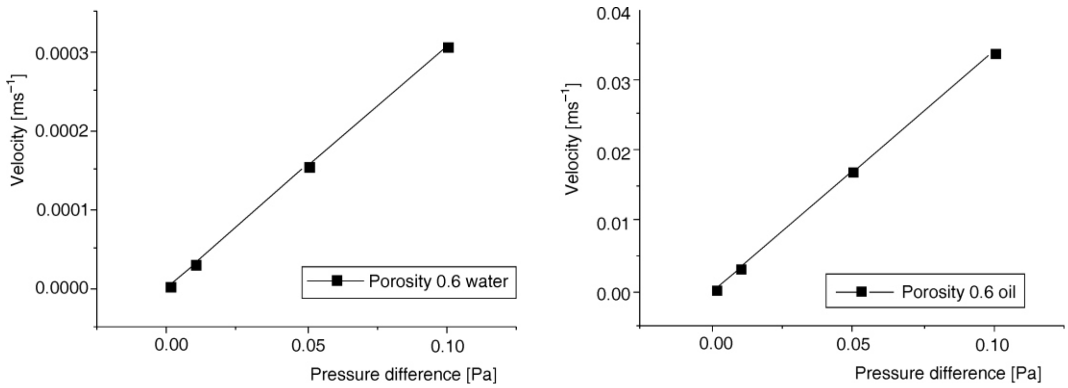

Figure 4. Average velocity variation of water/oil at different pressure difference

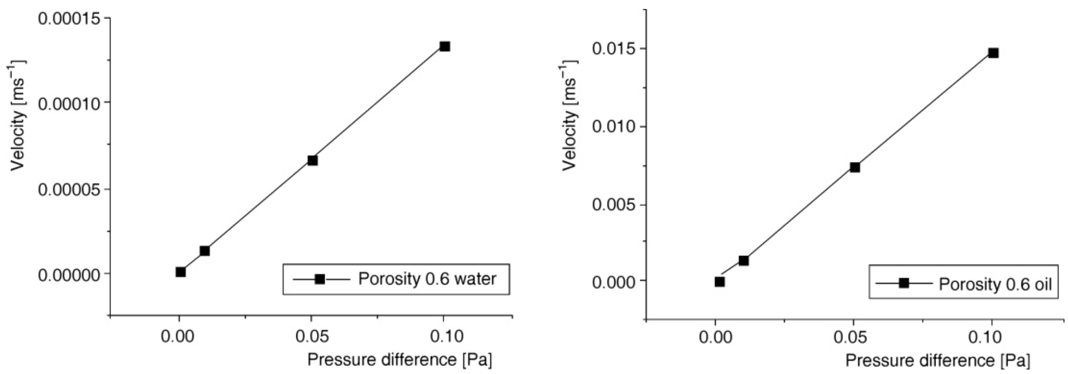

Figure 5. Average velocity variation of outlet face of water/oil at different pressure difference

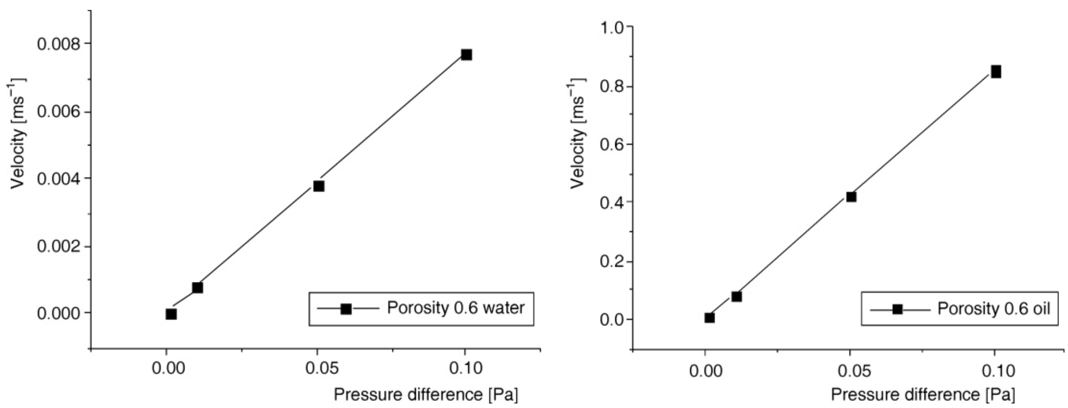

Figure 6. Maximum velocity variation of water/oil at different pressure difference

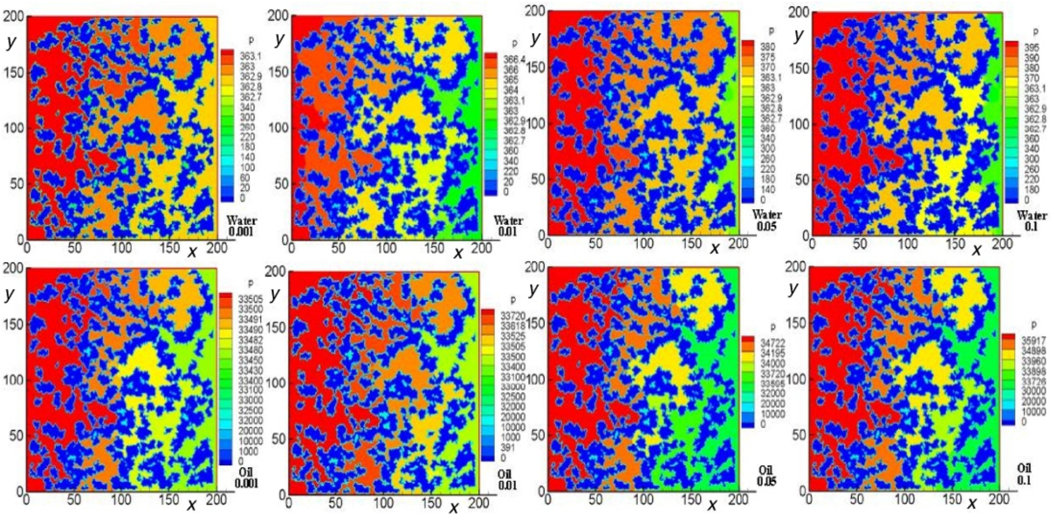

Figure 7. Pressure distribution contour for water/oil migration at different pressure difference

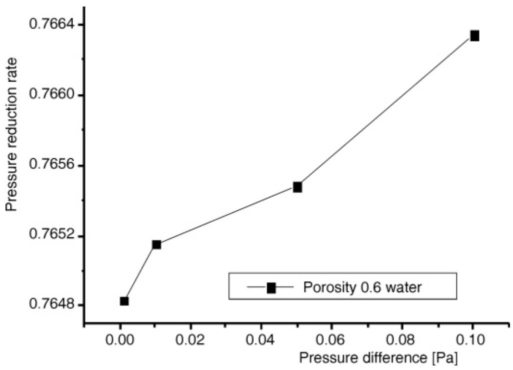

Figure 8. Pressure reduction rate curve at the inlet to maximum velocity point of water at different pressure difference

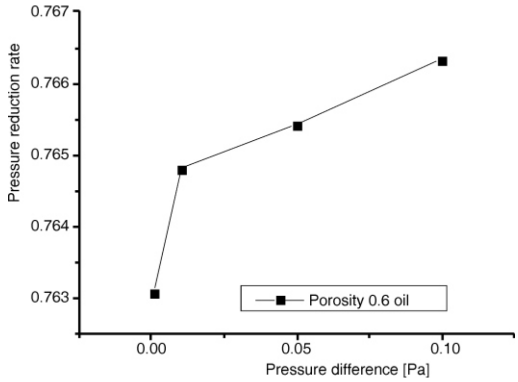

Figure 9. Pressure reduction rate curve at the inlet to maximum velocity point of oil at different pressure difference

main control point of the pressure is the inlet and outlet of the cavity. From the pressure nephogram, the pressure values of the maximum velocity point at different pressure are obtained, and the pressure reduction rate is shown in figs. 8 and 9.

As can be seen from figs. 8 and 9, as the pressure gradient increases, the pressure reduction rate increases gradually, but the change is smaller. The pressure reduction rate of water is about 76.48%, and the pressure reduction rate of oil is about 76.3%.

Oil and water resistance coefficient fitting

The porous medium at porosity 0.6 is chosen to obtain the drag coefficient. When the driving pressure difference is 0.001, 0.01, 0.05, and 0.1 (lattice unit), the average velocity (lat-

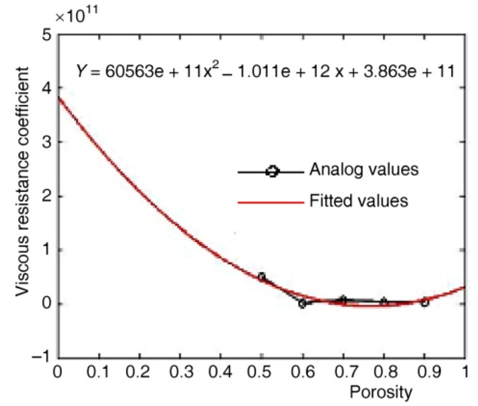

Figure 10. Distribution curve of water viscous resistance coefficient with porosity

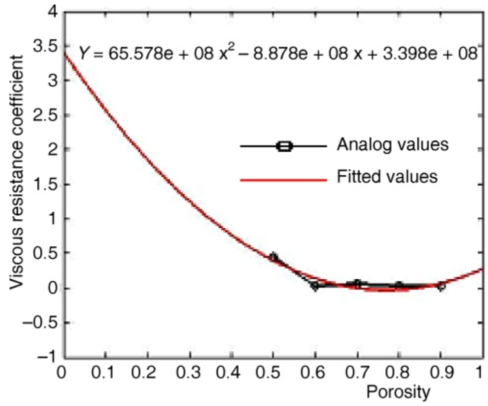

Figure 11. Distribution curve of oil viscous resistance coefficient with porosity

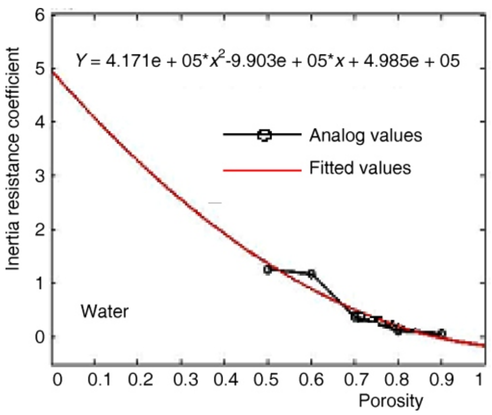

Figure 12. Distribution curve of water inertia resistance coefficient with porosity

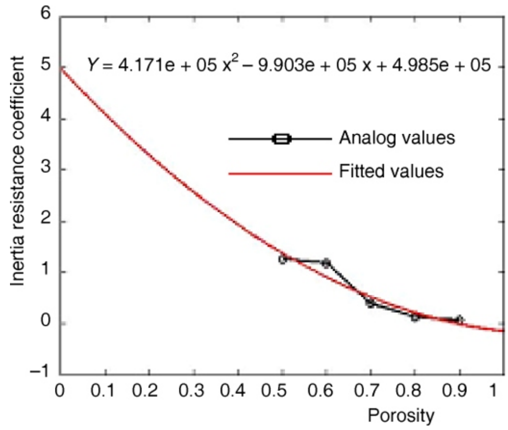

Figure 13. Distribution curve of oil inertia resistance coefficient with porosity

tice unit) of fluid in porous media is obtained. Then the lattice units are transformed into macroscopic physical units. According to the resistance coefficient acquisition model, taking the mean velocity of fluid in porous medium (macroscopic physical unit) as abscissa, the pressure (macroscopic physical unit) of unit length in left and right direction as ordinate, two time curves and equations are fitted. According to eqs. (13) and (14), the coefficients of viscous resistance and inertia resistance of porous medium are obtained.

When the fluid is water in porous medium, and a_1, a_2 are the coefficients of equation obtained by two time curve fitting method, and a1 is 0.24 10^7, a_2 is 5.88 10^7. According to eqs. (13) and (14), the viscous resistance coefficient and the inertia resistance coefficient of porous medium are obtained, and the viscous resistance coefficient is 2406779661, the inertia resistance coefficient is 117810.06. When the fluid is oil, and a_1 is 0.0023 10^7, a_2 is 4.94 10^7, and the viscous resistance coefficient is 2604166.67, the inertia resistance coefficient is 117811.16.

The resistance coefficients of porous media with different porosity are obtained according to the method of obtaining the resistance coefficient. Taking the porosity as the abscissa, and the viscous resistance coefficient and the inertia resistance coefficient as the ordinate, the two curve fitting methods are used to obtain the change curve of the drag coefficient with the porosity of the porous medium. The viscous resistance coefficients of oil and water are shown in figs. 10 and 11, and the inertia resistance coefficients are shown in figs. 12 and 13.

Comparing coefficients of oil and water resistance coefficient equations, it is obvious that the coefficient of viscous resistance is greater than the coefficient of inertia resistance. And the viscous resistance coefficient of water is greater than that of oil viscous resistance coefficient, and the coefficient of inertia resistance of oil and water is nearly same.

Conclusion

Through the simulation of oil and water migration in porous media, the equation of resistance coefficient of porous structure with different porosity was obtained. The conclusions are given as follows.

- When the same fluid passes through the porous medium, the coefficient of viscous resistance is greater than the coefficient of inertia resistance.
- When the different fluid passes through the porous medium, the viscous resistance coefficient of water is greater than that of oil, and the coefficient of inertia resistance of oil and water is nearly same.

Acknowledgment

The financial supports are provided by National Natural Science Foundation of China Grant No. 51534004 and Natural Science Foundation of Heilongjiang province Grant No. JJ2016ZR0314, the innovation reserve talent project of Heilongjiang province through Grant No. SCXHB201702, the National Science Foundation raising project through Grant No. NEPU201704 and the Postgraduate Innovation Research Project Grant No. YJSCX2017-024NEPU.

References

[1] Ma, Y., *et al.*, Simulation on the Spread Range of Oil Pipeline Leakage Soil (in Chinese), *Journal of Liaoning Shihua University, 32* (2012), 2, pp. 50-53
[2] Huang, S. L., *et al.*, Comparison of the Effect of Washing Diesel Oil-Contaminated Soil by Five Kinds of Surfactants (in Chinese), *Environmental Engineering, 33* (2015), 2, pp. 168-172
[3] Xiang, L., *et al.*, Influence of Chemical Flooding Technology on Environment (in Chinese), *Guangdong Chemical Industry, 44* (2017), 16, pp. 124-144
[4] Zang, F., *et al.*, Structure and Improvement of Filtration Device in Oilfield Water Treatment Equipment, *China New Technologies and New Products, 11* (2015), p. 69
[5] Zhang, N., *et al.*, Experimental Investigation on Resistance Characteristics of Two-Phase Flow through. Porous Media Channel, *Engineering of Nuclear Power, 32* (2011), 3, pp. 106-110
[6] Chen, P., *et al.*, Effect of Capillary Hysteresis on Two-Phase Flow in Porous Media (in Chinese), *Journal of Rock Mechanics and Engineering, 29* (2010), 10, pp. 2148-2158
[7] Yu, L. Z, *et al.*, Numerical Simulation of Single-Flow Resistance in Porous Media Channel, *Atomic Energy Science and Technology, 44* (2010), 12, pp. 1441-1444
[8] Kang, Q. J., *et al.*, Lattice Boltzmann Simulation of Chemical Dissolution in Porous Media, *Physical Review E*, *65* (2002), Mar., 036318
[9] Kang, Q. J., *et al.*, Lattice Boltzmann Pore-Scale Model for Multicomponent Reactive Transport in Porous media, *Journal of G eophysical Research: Solid Earth, 111* (2006), B5, pp. 1-9
[10] Kang, Q. J., *et al.*, An Improved Lattice Boltzmann Model for Multicomponent Reactive Transport in Porous Media at the Pore Scale, *Water Resources Research, 43* (2007), 12, pp. 2578-2584
[11] Song, W. Y., *et al.*, A Lattice Boltzmann Model for Heat and Mass Transfer Phenomena with Phase Transformations in Unsaturated Soil During Freezing Process, *International Journal of Heat and Mass Transfer, 94* (2016), Mar., pp. 29-38

[12] Song, W. Y., *et al*., Macroscopic Lattice Boltzmann Model for Heat and Moisture Transfer Process with Phase Transformation in Unsaturated Porous Media during Freezing Process, *Open Physics, 15* (2017), 1, pp. 379-393
[13] Bayat, M., *et al*., The Application of Lattice Boltzmann Method for Permeability Prediction of Porous Media: Investigating the Effects of Viscosity and Grid Resolution, *Petroleum Science and Technology, 30* (2012), 13, pp. 1324-1334
[14] Britta, N., *et al*., Combined Lattice Boltzmann and Phase-Field Simulations for Incompressible Fluid Flow in Porous Media, *Mathematics and Computers in Simulation, 80* (2010), 7, pp. 1458-1468
[15] Guo, Z., *et al*., A Coupled Lattice BGK Model for the Boussinesq Equations, *International Journal for Numerical Methods in Fluids, 39* (2002), 4, pp. 325-342
[16] Guo, Z. L., *et al*., Non-Equilibrium Extrapolation Method for Velocity and Pressure Boundary Conditions in the Lattice Boltzmann Method, *Chinese Physics, 11* (2002), 4, pp. 366-374
[17] Chen, S., *et al.*, On Boundary Conditions in Lattice Boltzmann Methods, *Physics of Fluids, 8* (1996), 9, pp. 2527-2536
[18] Wang, M., *et al*., Mesoscopic Predictions of the Effective Thermal Conductivity of Miroscale Random Porous Media, *Physical Review E, 75* (2007), 3, pp. 1324-1334

Paper submitted: October 11, 2017
Paper revised: November 12, 2017
Paper accepted: November 13, 2017